Office de la Propriété Intellectuelle du Canada
Un organisme d'Industrie Canada

Canadian Intellectual Property Office
An agency of Industry Canada

CA 2832184 A1 2012/10/11

(21) 2 832 184

(12) DEMANDE DE BREVET CANADIEN
CANADIAN PATENT APPLICATION

(13) A1

(86) Date de dépôt PCT/PCT Filing Date: 2012/04/06
(87) Date publication PCT/PCT Publication Date: 2012/10/11
(85) Entrée phase nationale/National Entry: 2013/10/02
(86) N° demande PCT/PCT Application No.: US 2012/032527
(87) N° publication PCT/PCT Publication No.: 2012/139002
(30) Priorité/Priority: 2011/04/07 (US61/516,738)

(51) Cl.Int./Int.Cl. *C07K 14/435* (2006.01), *C12N 15/62* (2006.01), *G01N 33/574* (2006.01)

(71) Demandeur/Applicant:
MEMORIAL SLOAN KETTERING CANCER CENTER, US

(72) Inventeurs/Inventors:
WENDEL, HANS-GUIDO, US;
ORCCHIO, ELISA, US

(74) Agent: SMART & BIGGAR

(54) Titre : COMPOSITIONS DE PROTEINE DE FUSION ANTICORPS ANTITUMORAL-SUPPRESSEUR DE TUMEUR ET PROCEDE D'UTILISATION POUR LE TRAITEMENT DU CANCER

(54) Title: ANTI-TUMOR ANTIBODY-TUMOR SUPPRESSOR FUSION PROTEIN COMPOSITIONS AND METHODS OF USE FOR THE TREATMENT OF CANCER

(57) Abrégé/Abstract:
The present invention is directed to methods and compositions for treating cancer, including, hematologic malignancies, such as B-cell malignancies, with anti-tumor antibody-tumor suppressor fusion proteins in order to selectively restore tumor suppressor gene function to cancer cells in which such tumor suppressor gene function has been lost. The present invention is also directed to methods and compositions for diagnosing cancer and for predicting and assessing response to treatment.

(12) INTERNATIONAL APPLICATION PUBLISHED UNDER THE PATENT COOPERATION TREATY (PCT)

(19) World Intellectual Property Organization
International Bureau

(43) International Publication Date
11 October 2012 (11.10.2012)

WIPO | PCT

(10) International Publication Number
WO 2012/139002 A3

(51) International Patent Classification:
A61K 47/48 (2006.01) *G01N 33/574* (2006.01)
C12N 15/62 (2006.01)

(21) International Application Number:
PCT/US2012/032527

(22) International Filing Date:
6 April 2012 (06.04.2012)

(25) Filing Language: English

(26) Publication Language: English

(30) Priority Data:
61/516,738 7 April 2011 (07.04.2011) US

(71) Applicant *(for all designated States except US)*: **MEMORIAL SLOAN-KETTERING CANCER CENTER** [US/US]; 1275 York Avenue, New York, NY 10065 (US).

(72) Inventors; and

(75) Inventors/Applicants *(for US only)*: **WENDEL, Hans-Guido** [DE/US]; 124 West 60th Street, Apt. 51a, New York, NY 10023 (US). **ORCCHIO, Elisa** [IT/US]; 504 East 81st Street, Apt. 5L, New York, NY 10028 (US).

(74) Agents: **HOWERTON, Thomas, C.** et al.; Medlen & Carroll, LLP, 703 Market Street, Suite 340, San Francisco, CA 94103 (US).

(81) Designated States *(unless otherwise indicated, for every kind of national protection available)*: AE, AG, AL, AM, AO, AT, AU, AZ, BA, BB, BG, BH, BR, BW, BY, BZ, CA, CH, CL, CN, CO, CR, CU, CZ, DE, DK, DM, DO, DZ, EC, EE, EG, ES, FI, GB, GD, GE, GH, GM, GT, HN, HR, HU, ID, IL, IN, IS, JP, KE, KG, KM, KN, KP, KR, KZ, LA, LC, LK, LR, LS, LT, LU, LY, MA, MD, ME, MG, MK, MN, MW, MX, MY, MZ, NA, NG, NI, NO, NZ, OM, PE, PG, PH, PL, PT, QA, RO, RS, RU, RW, SC, SD, SE, SG, SK, SL, SM, ST, SV, SY, TH, TJ, TM, TN, TR, TT, TZ, UA, UG, US, UZ, VC, VN, ZA, ZM, ZW.

(84) Designated States *(unless otherwise indicated, for every kind of regional protection available)*: ARIPO (BW, GH, GM, KE, LR, LS, MW, MZ, NA, RW, SD, SL, SZ, TZ, UG, ZM, ZW), Eurasian (AM, AZ, BY, KG, KZ, MD, RU, TJ, TM), European (AL, AT, BE, BG, CH, CY, CZ, DE, DK, EE, ES, FI, FR, GB, GR, HR, HU, IE, IS, IT, LT, LU, LV, MC, MK, MT, NL, NO, PL, PT, RO, RS, SE, SI, SK, SM, TR), OAPI (BF, BJ, CF, CG, CI, CM, GA, GN, GQ, GW, ML, MR, NE, SN, TD, TG).

[Continued on next page]

(54) Title: ANTI-TUMOR ANTIBODY-TUMOR SUPPRESSOR FUSION PROTEIN COMPOSITIONS AND METHODS OF USE FOR THE TREATMENT OF CANCER

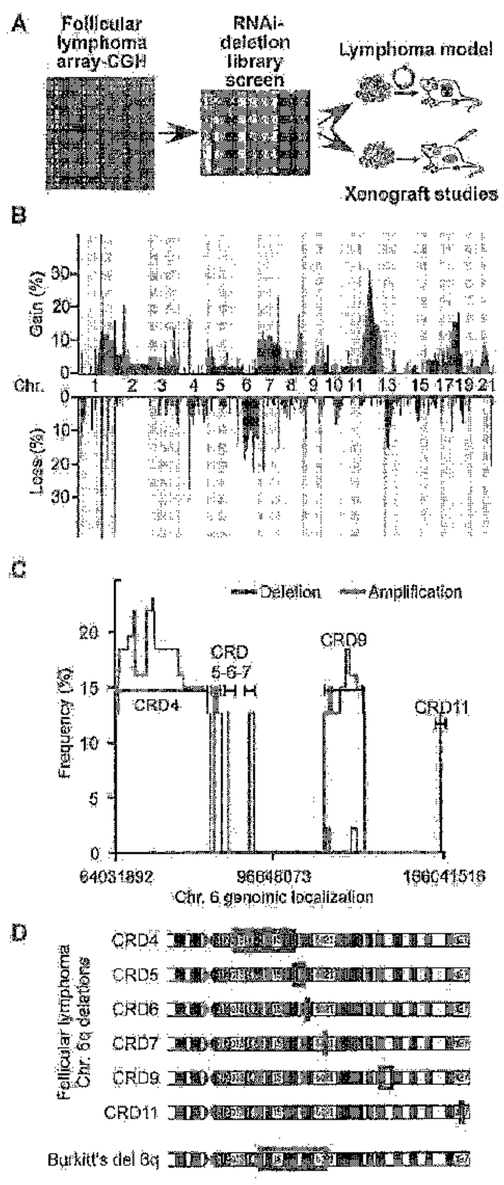


Figure 1

(57) Abstract: The present invention is directed to methods and compositions for treating cancer, including, hematologic malignancies, such as B-cell malignancies, with anti-tumor antibody-tumor suppressor fusion proteins in order to selectively restore tumor suppressor gene function to cancer cells in which such tumor suppressor gene function has been lost. The present invention is also directed to methods and compositions for diagnosing cancer and for predicting and assessing response to treatment.

WO 2012/139002 A3

WO 2012/139002 A3

Published:

— *with international search report (Art. 21(3))*

— *before the expiration of the time limit for amending the claims and to be republished in the event of receipt of amendments (Rule 48.2(h))*

(88) Date of publication of the international search report:
6 December 2012

Anti-Tumor Antibody-Tumor Suppressor Fusion Protein Compositions And Methods Of Use For The Treatment Of Cancer

CROSS-REFERENCE TO RELATED APPLICATIONS

This application claims priority under 35 U.S.C. §119(e) to co-pending U.S. Provisional Application Serial No. 61/516,738, filed on April 7, 2011, herein incorporated by reference in its entirety.

GOVERNMENT INTEREST

This invention was made with government support under CA142798-01 awarded by the National Institutes for Health (NIH). The government has certain rights in the invention.

FIELD OF THE INVENTION

The present invention is directed to methods and compositions for treating cancer, including, specifically, hematologic malignancies, and including, more specifically, B-cell malignancies, with anti-tumor antibody-tumor suppressor fusion proteins in order to selectively restore tumor suppressor gene function to cancer cells in which such tumor suppressor gene function has been lost. The present invention is also directed to methods and compositions for diagnosing cancer and for predicting and assessing response to treatment.

BACKGROUND OF THE INVENTION

Conventional approaches to treating malignancies and to predicting and assessing their responses to specific treatment regimens rely on properly classifying the type of tumor present. Proper classification, in turn, relies primarily on clinical features, tumor cell morphology, tumor cell immunophenotype and, to a lesser extent, tumor cell chromosomal abnormalities. However, even within a given tumor type, response to specific treatment regimens is, often, quite variable, and analyses at the molecular level reveal that the tumor types defined by conventional classification schemes are, often, quite heterogeneous.

Recent efforts to classify tumors, including hematologic malignancies, have, therefore, focused on identifying the specific genetic abnormalities that drive the growth of specific tumor types. Such genetic abnormalities can then serve as markers of disease and/or as targets for therapy.

Follicular lymphomas (FLs) are among the most common B-cell malignancies. FLs are characterized by a t(14;18)(q32;q21) chromosomal translocation that results in constitutive expression of the anti-apoptotic B-cell CLL/lymphoma 2 (Bcl2) protein. However, lymphomagenesis and disease progression require additional genetic lesions (Bende, Smit and van Noesel 2007). Amplification of *c-MYC*, loss of *p53* and deletions of chromosome 6q have all been associated with progression of B-cell lymphomas and shortened survival (Johnson, et al. 2009) (Nanjangud, et al. 2007). The exact nature of these molecular events is only incompletely understood. Clinical outcome for patients with B-cell lymphomas has improved with the addition of anti-CD20 antibody (e.g., rituximab) to conventional chemotherapeutic regimens. However, transplantation remains the only curative option for FL (Relander, et al. 2010).

Recent technological advances have facilitated the genome-wide detection of genetic and epigenetic changes in cancer. In parallel, RNA-interference (RNAi) technology and its adaptation to genetic screens have enabled the execution of rapid and unbiased loss-of-function studies in mammalian cells and *in vivo* (McCaffrey, et al. 2002). Together, these technologies can help uncover tumor suppressor genes that might not have been identified by genomic data analyses alone (Oricchio, et al. 2010).

The protein products of tumor suppressor genes can directly or indirectly prevent cell division or lead to cell death. Functional loss of tumor suppressor genes and/or their protein products through gene deletion, inactivating mutation or epigenetic mechanisms can result in uncontrolled cell growth and the development of cancer. Many tumors are known to result primarily from the functional loss of a tumor suppressor. However, due to the difficulties inherent in targeting tumor suppressor function specifically to those cancer cells in which such tumor suppressor function has been lost, restoration of tumor suppressor function to tumor cells has not, heretofore, been viewed as a practicable approach to the treatment of cancer.

SUMMARY OF THE INVENTION

This invention is drawn to methods and compositions for diagnosing and treating cancer, including B-cell malignancies, and for predicting and assessing response to treatment. In some embodiments, deletion of the ephrin receptor A7 gene (*EPHA7*) or loss of EphA7 expression can be used to identify a subset of lymphomas that will respond to treatment with a secreted, truncated EphA7 isoform comprising the extracellular domains of EphA7 ($EphA7^{ECD}$; sometimes referred to as $EphA7^{TR}$) or analogues thereof. In other embodiments, administration of a pharmaceutical composition comprising an anti-CD20 antibody-$EphA7^{ECD}$ fusion protein (anti-CD20-EphA7), in which $EphA7^{ECD}$ is fused downstream of the rituximab (Rituxan®/MabThera®) immunoglobulin G1 (IgG1) constant region, can be used to treat such lymphomas. In some other embodiments, deletion of *EPHA7*, loss of EphA7 expression and/or increased cell surface expression of EphA receptors, including EphA2, can be used to identify tumors likely to respond to treatment with $EphA7^{ECD}$ or analogues thereof. In yet other embodiments, administration of a pharmaceutical composition comprising an anti-tumor antibody-$EphA7^{ECD}$ fusion protein can be used to treat such tumors.

Thus, in one embodiment, the invention provides an anti-tumor antibody-tumor suppressor fusion protein comprising: (1) a recombinant immunoglobulin (Ig) heavy chain or portion thereof having an amino-terminal variable region (Fv) specific for a cell-surface antigen of a tumor cell; and (2) said heavy chain or portion thereof being joined at its carboxy-terminus by a peptide bond to the amino-terminal amino acid of a tumor suppressor protein or functional portion thereof. In one embodiment, the Ig heavy chain of the anti-tumor antibody-tumor suppressor fusion protein comprises the Fv of rituximab. In another embodiment, the Ig heavy chain Fv of the anti-tumor antibody-tumor suppressor fusion proteinis specific for CD20. In a particular embodiment, the Ig heavy chain Fv is specific for a cell-surface antigen found on malignant B-cells. In a further embodiment, the Ig heavy chain Fv is specific for a cell-surface antigen found on the cells of a hematologic tumor. In another embodiment, the Ig heavy chain Fv is specific for a cell-surface antigen of the cells of a solid tumor. In another embodiment, the

tumor suppressor protein is EphA7^{ECD}. In yet a further embodiment, the tumor suppressor protein is EphA7 or an EphA2-binding portion thereof.

The invention also provides a method for treating cancer comprising administering a therapeutically effective amount of any one or more of the anti-tumor antibody-tumor suppressor fusion proteins described herein.

The invention additionally provides a DNA construct or constructs encoding any one or more of the anti-tumor antibody-tumor suppressor fusion proteins described herein.

Also provided by the invention is a tumor suppressor immunoconjugate comprising: (1) a recombinant Ig heavy chain or portion thereof having an Fv specific for a cell-surface antigen of a tumor cell joined at its carboxy-terminus by a peptide bond to the amino-terminal amino acid of a tumor suppressor protein or functional portion thereof; and (2) an Ig light chain or portion thereof having an Fv specific for said cell-surface antigen, said Ig heavy and light chains or portions thereof forming together a functional antigen-binding site, such that said immunoconjugate displays both antigen-binding specificity and tumor suppressor activity.

The invention further provides a method for treating cancer comprising administering a therapeutically effective amount of any one or more of the tumor suppressor immunoconjugates described herein. In one embodiment, the antigen-binding site is the antigen-binding site of rituximab. In another embodiment, the antigen-binding site is specific for CD20. In a further embodiment, the antigen-binding site is specific for a cell-surface antigen found on malignant B-cells. In another embodiment, the antigen-binding site is specific for a cell-surface antigen found on the cells of a hematologic tumor. In yet an alternate embodiment, the antigen-binding site is specific for a cell-surface antigen of the cells of a solid tumor. In a further embodiment, the tumor suppressor protein is EphA7^{ECD}. In an alternative embodiment, the tumor suppressor protein is EphA7 or an EphA2-binding portion thereof.

The invention additionally provides a DNA construct or constructs encoding any one or more of the tumor suppressor immunoconjugates described herein.

The invention further provides a method to identify tumors responsive to treatment with any one or more of the anti-tumor antibody-tumor suppressor fusion proteins described herein, by measuring the deletion or inactivation of the gene for said tumor suppressor and/or the loss of expression of said tumor suppressor protein. In one embodiment, the tumor suppressor protein is $EphA7^{ECD}$.

Also provided by the invention is a method to identify tumors responsive to treatment with any one or more of the tumor suppressor immunoconjugates described herein, by measuring the deletion or inactivation of the gene for said tumor suppressor and/or the loss of expression of said tumor suppressor protein. In a particular embodiment, the tumor suppressor protein is $EphA7^{ECD}$.

The invention also provides a method to identify tumors responsive to treatment with any one or more of the anti-tumor antibody-tumor suppressor fusion proteins described herein, by measuring cell-surface EphA receptor expression.

Also provided by the invention is a method to identify tumors responsive to treatment with any one or more of the tumor suppressor immunoconjugates described herein, by measuring cell-surface EphA receptor expression.

The invention further provides a fusion protein comprising a recombinant immunoglobulin (Ig) heavy chain or portion thereof having an amino-terminal variable region (Fv) that specifically binds to a tumor cell surface marker antigen, wherein the Ig heavy chain or portion thereof is linked at its carboxy-terminus by a peptide bond to the amino-terminal amino acid of tumor suppressor protein $EphA7^{ECD}$. In one embodiment, the tumor suppressor protein $EphA7^{ECD}$ comprises SEQ ID NO: 02.

The invention also provides a recombinant expression vector comprising a nucleotide sequence encoding a fusion protein comprising a recombinant immunoglobulin (Ig) heavy chain or portion thereof having an amino-terminal variable region (Fv) that specifically binds to a tumor cell surface marker antigen, wherein the Ig heavy chain or portion thereof is linked at its

carboxy-terminus by a peptide bond to the amino-terminal amino acid of tumor suppressor protein EphA7ECD.

The invention additionally provides a method for reducing one or more symptoms of cancer comprising administering to a subject in need thereof a therapeutically effective amount of at least one of (a) a fusion protein comprising a recombinant immunoglobulin (Ig) heavy chain or portion thereof having an amino-terminal variable region (Fv) that specifically binds to a tumor cell surface marker antigen, wherein the Ig heavy chain or portion thereof is linked at its carboxy-terminus by a peptide bond to the amino-terminal amino acid of tumor suppressor protein EphA7^{ECD}, and (b) a recombinant expression vector comprising a nucleotide sequence encoding a fusion protein comprising a recombinant immunoglobulin (Ig) heavy chain or portion thereof having an amino-terminal variable region (Fv) that specifically binds to a tumor cell surface marker antigen, wherein the Ig heavy chain or portion thereof is linked at its carboxy-terminus by a peptide bond to the amino-terminal amino acid of tumor suppressor protein EphA7ECD. In one embodiment, the cancer is lymphoma. In another embodiment, the cancer comprises cancer cells that a) express CD20 protein, and b) comprise one or more of i) deletion of ephrin receptor A7 (*EPHA7*) gene, ii) reduced expression of EphA7 protein, and iii) increased expression of EphA2 protein. In a further embodiment, the cancer cells comprise B cells. In a particular embodiment, the cancer is lymphoma. In a more particular embodiment, the subject is human.

In the present disclosure, the invention is described with reference to specific embodiments thereof. It will, however, be evident that various modifications and changes may be made thereto without departing from the broader scope and spirit of the invention. The summary, description, materials and methods and drawings are, accordingly, to be regarded in an illustrative rather than restrictive sense.

Numerous references have been made to patents and printed publications throughout this document. Each of the cited references and printed publications is individually incorporated herein by reference in its entirety.

DETAILED DESCRIPTION OF THE INVENTION

Introduction

FLs are among the most common types of non-Hodgkin's lymphoma (NHL). They are characterized by the translocation t(14;18)(q32;q21) and increased expression of *BCL2* (Bende, Smit and van Noesel 2007). Amplification of *c-MYC*, loss of *p53* and deletions of chromosome 6q have all been associated with progression and shortened survival in FL (Nanjangud, et al. 2007). Up to 20% of FLs sustain large and hemizygous deletions of chromosome 6q11-27, suggesting the presence of one or more tumor suppressor genes in this region (Offit, et al. 1993) (Gaidano, et al. 1992). Clinically, FL shows persistent growth and eventual progression. Outcomes have improved with the addition of the anti-CD20 antibody rituximab to standard chemotherapeutic regimens, but transplantation remains the only curative option for FL (Relander, et al. 2010).

We used an unbiased loss-of-function screen to complement genomic analyses of tumors. Using an RNAi library tailored to the 6q deletions seen in FL, we identified a secreted form of the EphA7 receptor ($EphA7^{ECD}$) (Holmberg, Clarke and Frisén 2000) as a tumor suppressor. Hemizygous loss of *EPHA7* occurs in 12% of FLs, and the gene is differentially silenced in up to 72% of FLs. *In vivo* knockdown of *EPHA7* accelerates lymphoma development in mouse models of FL. Conversely, the purified $EphA7^{ECD}$ protein has striking anti-tumor effects on xenografted human lymphoma cells. Moreover, by fusing EphA7 to an anti-CD20 antibody, we are able to target EphA7's tumor suppressive activity to $CD20^{+}$ lymphoma cells *in vivo*. Thus, we identify a surprising role for $EphA7^{ECD}$ as an antitumor protein with significant therapeutic potential in lymphoma, and we describe a new strategy, use of anti-tumor antibody-tumor suppressor fusion proteins, to selectively restore tumor suppressor gene function to cancer cells in which such function has been lost.

Genomic Analysis of 6q Deletions in FL and Burkitt's Lymphoma (BL)

We conducted a systematic functional genomics study into the molecular pathogenesis of FL (Figure 1a). First, we analyzed 64 FLs representing pathological grades I-III (Grade I, 21; II, 23;

IIIa, 16; IIIb, 8) by array-comparative genomic hybridization (aCGH). We observed 92 common (i.e., present in more than 10% of FLs tested) regions of deletion (CRD); 38 were tumor-specific and not found in the reference DNA, four were physiological and 50 were copy number variations (CNVs) (Figure 1b). Consistent with previous cytogenetic studies (Offit, et al. 1993) (Gaidano, et al. 1992) (Hauptschein, et al. 1998), we found that deletions affecting chromosome 6q11-27 occurred in 23% of FLs (15/64 cases). Individual cases showed a heterogeneous pattern of 6q loss (Figure 2).

Cumulative analyses revealed CRDs that ranged from 5 kilobases (kb) (CRD11) to 27 megabases (Mb) (CRD4) and harbored between one and 78 genes (Figure 1c and 1d). Almost all the deletions were hemizygous, and small regions of apparent homozygous loss within CRD4 and CRD11 did not affect any genes. Analysis of six HIV-associated Burkitt's lymphomas (BLs) revealed partially overlapping 6q deletions in two cases (Figure 1d, Figure 3). Thus, while the size and complex patterns of hemizygous 6q deletions in FL suggest the presence of multiple tumor suppressor genes in this region, genomic data alone do not directly pinpoint a specific tumor suppressor gene.

Unbiased RNAi Screen Identifies *EPHA7* as a Tumor Suppressor Gene in 6q11-27

Given the complexity of 6q deletions in FL, we wondered whether an unbiased deletion-specific loss-of-function screen could point to potential tumor suppressor genes. We constructed a library of 260 short hairpin RNAs (shRNAs) targeting 84 genes (1 - 7 shRNAs per gene) in a murine stem cell virus (MSCV)-based, green fluorescent protein (GFP)-expressing vector. We used non-transformed murine pro-B lymphocytes (FL5-12 cells) engineered to express increased levels of Bcl2 as a surrogate *in vitro* system and screened for shRNAs that protect cells from cytokine (interleukin-3; IL-3) depletion (Mavrakis, et al. 2010) (Figure 4a). Briefly, we partially transduced FL5-12 cells overexpressing Bcl2 with the pooled 6q deletion library or empty vector and monitored for enrichment of cells expressing GFP (and shRNAs) following IL-3 depletion (Figure 4b). Sequencing identified the shRNAs present in the enriched population (Figure 4c), and individual re-testing confirmed a protective effect for shRNAs targeting the tumor necrosis factor, alpha-induced protein 3 (*TNFAIP3*; A20) and *EPHA7* genes (Figure 4d,

Figures 5 and 6). Hence, our RNAi screen identifies a known tumor suppressor (*TNFAIP3)* (Compagno, et al. 2009) and points to E*PHA7* as a new candidate tumor suppressor gene.

In Vivo Knockdown of _EPHA7_ Accelerates Lymphoma Development in Mouse Models of FL

Next, we tested the effect of *EPHA7* in a mouse model of FL. Briefly, the vavP-*BCL2* model recapitulates the genetics and morphology of human FL (Egle, et al. 2004). We transduced vavP-*BCL2* transgenic hematopoietic progenitor cells (HPCs) with retroviral shRNA constructs and transplanted these genetically engineered cells into irradiated recipients (Wendel, et al. 2004) (Figure 4e). Ninety percent of control animals remained tumor free for more than 100 days (vector; n = 11). *c-MYC* and *p53* have established roles in FL transformation (Nanjangud, et al. 2007), and enforced *c-MYC* expression ($p < 0.01$; n = 7) and *p53* knockdown (median survival 60 days, $p < 0.01$; n = 9) both accelerated lymphomagenesis *in vivo*. *EPHA7* knockdown had an effect on tumor latency similar to that of *p53* knockdown ($p < 0.01$; n = 18) (Figure 4f). Knockdown of *TNFAIP3* alone or in combination with knockdown of *EPHA7* in the vavP-*BCL2* model showed modest effects on lymphoma latency [$p_{(TNFAIP3 \text{ vs. vector})} = 0.28$; n = 3 and $p_{(TNFAIP3+EPHA7 \text{ vs. } EPHA7)} = 0.93$; n = 5)] (Figure 7). Analysis of tumors induced in vavP-*BCL2* mice revealed features of FLs. These included follicular structures and peanut agglutinin (PNA) positivity, consistent with a germinal center (GC) B-cell phenotype. The lymphomas had overall low but heterogeneous Ki67, while apoptosis was absent. Only the vavP-*BCL2/c-MYC* tumors grew in a diffuse pattern resembling diffuse large B-cell lymphoma (DLBCL) (Figure 4g, Figure 8). All the tumors expressed B-cell markers (B220, CD19), and exhibited varying degrees of T-cell infiltration (Egle, et al. 2004). Sequencing of the immunoglobulin JH4 intron confirmed somatic hypermutation (Mandelbaum, et al. 2010) (Egle, et al. 2004) (McBride, et al. 2008). Polymerase chain reaction (PCR) analysis of the immunoglobulin heavy chain locus in tumors confirmed their clonal origin (Figure 9) (Egle, et al. 2004). Immunoblots revealed EphA7 expression in murine splenocytes and HPCs and partial knockdown in lymphomas (Figure 9d and 9e, Figure 10). Thus, *EPHA7* behaves as a tumor suppressor gene in a murine model that recapitulates many aspects of the genetics and pathology of FL.

We made similar observations regarding EphA7 in the Eμ-*MYC* model of pre-B-cell lymphoma (Adams, et al. 1985). Knockdown of *EPHA7* (n = 11) accelerated tumor development compared to vector ($p < 0.001$; n = 60) (Figure 10).

EPHA7 is Inactivated by Deletion and/or Promoter Methylation in Lymphoma

EPHA7 is affected by hemizygous deletions in 12% of FL, and we wondered whether *EPHA7* might also be subject to epigenetic silencing or mutational inactivation. We noted a differential reduction of *EPHA7* expression levels in lymphoma cells compared to GC B-cells (Figure 11a and 11b). We did not detect *EPHA7* mutations in FL. However, quantitative reverse transcription-PCR (qRT-PCR) revealed decreased *EPHA7* mRNA levels in purified lymphoma cells. Specifically, 41 of 50 FLs (82%) and four of six BLs (67%) exhibited decreased *EPHA7* mRNA levels compared to B-cells from GC or tonsils ($p_{(\text{lymphoma vs. B-cell})} < 0.02$) (Figure 3a). Similarly, the EphA7 protein was easily detected in normal tonsils by immunohistochemistry but completely absent in 231 of 332 FL samples (72%) on a tissue microarray (TMA) (Figure 11b and 11c and Figure 12).

Mass spectrometric analysis (MassARRAY) of the *EPHA7* promoter in 32 primary FLs and 16 lymphoma cell lines revealed extensive CpG island methylation consistent with epigenetic gene silencing (Figure 11d and 11e). Analysis of a second panel of cells using the HpaII tiny fragment enrichment by ligation-mediated PCR (HELP) assay for methylation detection confirmed differential methylation of the *EPHA7* promoter in lymphoma cells (9 FLs, 155 DLBCLs and 24 lymphoma cell lines) vs. GC B-cells (n = 9), the normal counterpart of the lymphomas tested (Figure 13). Concordantly, *in vitro* treatment of human lymphoma cells with 5-aza-2'-deoxycytidine caused re-expression of *EPHA7* (Figure 11f, Figure 14). The effect was less pronounced in Raji cells, which have only one copy of the *EPHA7* gene (Figure 15). Thus, loss of *EPHA7* expression in lymphomas is due to differential methylation of the *EPHA7* promoter.

Consistent with our observations, differential silencing of *EPHA7* has been reported in murine lymphomas and human B-lymphoblastic leukemias (B-ALLs) (Dawson, et al. 2007) (Kuang, et al. 2010). Hence, evidence of differential epigenetic silencing supports the role of *EPHA7* as a tumor suppressor gene in B-cell malignancies.

B-cells Express Only A Secreted, Truncated Isoform Comprising the Extracelluar Domains of EphA7

Ephrin receptors are tyrosine kinases that form dimers and are activated upon contact with ephrin-expressing cells (Seiradake, et al. 2010) (Himanen, et al. 2010). The role of ephrin signaling in cancer is unclear; both oncogenic and tumor suppressive functions have been proposed (Noren, et al. 2006) (Pasquale 2010). Alternate splicing of *EPHA7* produces a truncated protein (designated $EphA7^{ECD}$ or $EphA7^{TR}$), which lacks the intracellular domains and the kinase activity of the full-length protein (Holmberg, Clarke and Frisén 2000) (Dawson, et al. 2007) (Valenzuela, et al. 1995). Murine B-lymphocytes and 5-aza-2'-deoxycytidine-treated SU-DHL-10 cells express only $EphA7^{ECD}$ (Figure 16a, Figure 14), which is shed into the media (Figure 16a).

$EphA7^{ECD}$ Binds to EphA2, Blocking Activation of EphA2 and Src Kinases

Immunoprecipitation of immunoglobulin Fc fragment-tagged $EphA7^{ECD}$ ($EphA7^{Fc}$) demonstrates binding of EphA7 to the EphA2 receptor in Raji (Figure 16b) and FL-derived DoHH2 cells (Figure 17a). Enzyme-linked immunosorbent assay (ELISA) reveals inhibition of EphA2 phosphorylation by $EphA7^{Fc}$ (Figure 16c). Both knockdown of EphA2 and administration of $EphA7^{Fc}$ protein block Erk activation in Raji cells (Figure 16d and 16e) and in SU-DHL-6, DoHH2 and Karpas 422 cells (Figure 17c and 17d). Unlike tumor cells, the non-transformed FL5-12 lymphocytes express $EphA7^{ECD}$. Knockdown of *EPHA7* in FL5-12 cells activates Erk, and this activation is reversed upon treatment of the cells with $EphA7^{Fc}$ (Figure 18). A phosphoprotein array identifies additional signaling effects of $EphA7^{Fc}$ in Raji cells (Figure 19a and 19b). We confirmed effects on Erk, STAT3 and Src phosphorylation by immunoblot and note some differences between different lymphoma lines (Figure 16e, Figure 19d and 19e).

We modeled the interaction between EphA7 and EphA2 based on the known structure of EphA2 (Seiradake, et al. 2010) (Himanen, et al. 2010) and its homology with the EphA7 sequence (51%) and domain structure. Our model suggests an interaction through the receptors' Sushi and ligand binding domains (Figure 16f) suggesting that $EphA7^{ECD}$ and $EphA7^{Fc}$

function as decoy receptors, dimerizing with EphA2 on the cell surface and inhibiting EphA2 activation and signaling. More generally, our model suggests that EphA7^{ECD} and EphA7^{Fc} can dimerize with other EphA receptors on the cell surface and inhibit their activation and signaling as well.

EphA7^{Fc} Exhibits Anti-Tumor Activity *In Vitro* and *In Vivo*

Restoration of *EPHA7* activity, by retroviral transduction or application of EphA7^{Fc}, has anti-proliferative effects against Raji, SU-DHL-10, DoHH2 and Karpas 422 cells *in vitro* (Figures 20 and 21). Intravenous administration of purified EphA7^{Fc} (20µg/day for 3 days) resulted in dramatic regression of xenografted Raji and SU-DHL-10 tumors while vehicle (i.e., Fc)-treated tumors continued to grow (n = 12; $p_{(EphA7Fc\ vs.\ Fc)}$ <0.04) (Figure 16g, Figure 22). Residual Eph7^{Fc}-treated Raji tumors exhibited extensive apoptosis, disrupted architecture and reduced Erk phosphorylation (Figure 16h - j). Systemic administration of EphA7^{Fc} in a prevention study (20µg/day intravenously for 3 days) was well tolerated and significantly delayed development of Raji lymphomas (EphA7^{Fc}, n = 5; Fc, n = 5; p <0.05) (Figure 16k). EphA7^{Fc} treatment of other tumor cell lines expressing high levels of cell-surface EphA2, including some breast cancer cell lines, resulted in significant inhibition of EphA2 signaling as assessed by Erk phosphorylation.

Anti-Lymphoma Activity of Anti-CD20-EphA7^{ECD} Fusion Antibody Surpasses That of Anti-CD20 Antibody or EphA7^{ECD}

Next, we tested whether fusing EphA7^{ECD} to an anti-CD20 antibody (rituximab) could further enhance the therapeutic potential of EphA7^{ECD} (Figure 16l, Figure 23a). The fusion antibody (anti-CD20-EphA7) retains properties of both proteins. It recognizes CD20^{+} lymphoma cells and blocks EphA2 and Erk phosphorylation (Figure 16m, Figure 23b and 23c). The fusion antibody was also more efficient than anti-CD20 alone in slowing proliferation of, and killing, Raji or DoHH2 cells *in vitro* (Figure 16n and 16o, Figure 24). *In vivo* treatment with either anti-CD20 or anti-CD20-EphA7 (1µg/day intravenously for 5days) was well tolerated. In Raji xenografts (>1cm^3 at time of treatment), administration of low-dose anti-CD20 antibody produced partial responses or slowed progression compared to vehicle (Fc). Only the fusion antibody produced

complete responses (*ex vivo* tumor weight 0 – 30 mg) in 3 of 7 animals (p = 0.039, Fisher's exact for all three groups) (Figure 16p, Figure 25). Thus, anti-tumor antibodies can be used to selectively restore tumor suppressor function to cancer cells in which such function has been lost.

MATERIALS AND METHODS

Array-Comparative Genomic Hybridization (a-CGH)

DNA from fresh frozen or optimal cutting temperature compound-embedded tissue was isolated by the standard phenol-chloroform extraction method. DNA was quantified using a NanoDrop spectrophotometer (Thermo Fisher Scientific Inc.; www.nanodrop.com), its purity assessed by the ratio of absorptions at 260 nm vs. 280 nm and its integrity visualized on a 1% agarose gel with ethidium bromide. Prior to labeling each DNA sample and hybridizing it to an Agilent (Agilent Technologies; www.agilent.com) 244K oligonucleotide array, digestion efficiency was checked by incubating 1 µg of DNA with 1 µl of HaeIII restriction enzyme (10 U/µl) at 37°C for 2 hours and running the undigested and digested DNA (100 ng each) on a 1% agarose gel in parallel with a 1 kb DNA ladder. Human male DNA obtained from Promega Corporation (www.promega.com; Catalog# G147A) served as the reference DNA. Labeling and hybridization were performed according to protocols provided by Agilent. The slides were analyzed at 5 µm resolution using the Agilent G2565 Microarray Scanner System and Agilent Feature Extraction software (v9.1).

DNA Copy Number Analysis

With the exception of Figure 16, which uses the UCSC March 2006 human reference sequence (hg18/NCBI Build 36), all genomic positions described in this study refer to UCSC May 2004 human reference sequence (hg17/NCBI Build 35) (http://genome.ucsc.edu/cgi-bin/hgGateway). The modified Circular Binary Segmentation (CBS) algorithm was used to identify segmental gains and losses along the autosomes. Change-points were defined as segments, corresponding to p-values <0.05. A CRD was defined as a gain and/or loss of two contiguous probes observed in >10% of the cases. A total of 92 CRDs were identified. Of these, four were physiological

changes (B- and T-cell receptors), 50 were CNVs and the remaining 38 were tumor-specific. The Database of Genomic Variants (DGV), a catalogue of structural variations curated by The Centre for Applied Genomics (TCAG) (http://projects.tcag.ca/variation/) was used to identify and exclude CNVs. At the time of data analysis, the DGV comprised 8,083 entries that mapped to 3,933 genomic loci [variation.hg17.v2.txt; September 5, 2007 (Build 35/hg17)]. CGH data was further processed using Agilent's Feature Extraction software to quantitate the images. For normalization, we used a custom GC-normalization algorithm, which does a loess norm on both the total intensity of the probes and the local GC content in the genomic region surrounding the probes. The normalized data were segmented using DNAcopy, the standard CBS algorithm available from Bioconductor (http://www.bioconductor.org/help/bioc-views/release/bioc/html/DNAcopy.html). Each sample was then normalized to its own per-sample noise by dividing the segment means by the derivative noise (the mean absolute values of the difference between adjacent probes on the arrays). The next step used the RAE algorithm (Taylor, et al. 2008) to do a multi-sample analysis of the entire cohort. The RAE algorithm computes per-sample-calibrated thresholds, which can be used to compare signal levels across samples. The threshold function converts the log2 ratio signals from the CBS output via two logistic functions to a loss [-1,0] and gain [0-1] indicator output that is then averaged to give the genome-wide gain/loss recurrence frequency (plotted in Figure 1). For the chromosome 6q loss analysis, we used a global threshold of -0.5 for loss and 4.5 for homozygous deletion. Figure 3 shows the segment boundaries as computed by CBS with the vertical axis indicating the magnitude of the segment mean. See Taylor, et al. (2008) for additional details.

Molecular Analysis of Murine Tumors

Genomic DNA was extracted from the lymphomas arising in transgenic vavP-*BCL2* mice and from the lymphomas derived from transplanted vavP-*BCL2* HSC. For DNA extraction, frozen tissue was submerged in liquid nitrogen then pulverized. The resulting powder was collected and transferred to a microfuge tube on ice. DNA was purified using the Gentra Puregene Cell Kit (Qiagen; www.qiagen.com) and diluted in water, and DNA quality was assessed by

visualization after electrophoresis in a 1% agarose gel. DJ recombination in murine tumors was analyzed by nested PCR as described (Yu and Thomas-Tikhonenko 2002), and samples were analyzed using an Agilent 2100 Bioanalyzer and DNA 1000 Kit. For analysis of somatic hypermutation analyses, DNA samples were amplified as described (McBride, et al. 2008), and the PCR products were directly sequenced exactly as reported (Mandelbaum, et al. 2010).

Quantitative DNA Methylation Analysis

Quantitative DNA methylation analysis was carried out using MassARRAY EpiTYPER from Sequenom, Inc. (www.sequenom.com). The MassARRAY EpiTYPER is a tool for the detection and quantitative analysis of DNA methylation using base-specific cleavage of bisulfite-treated DNA and Matrix-Assisted Laser Desorption/Ionization Time-of-Flight Mass Spectrometry (MALDI-TOF MS). Specific PCR primers for bisulfite-converted DNA were designed using Sequenom's EpiDesigner program (www.epidesigner.com). T7-promoter tags were added to the reverse primer to obtain a product that could be transcribed *in vitro*, and a 10-mer tag was added to the forward primer to balance the PCR conditions. Unmethylated cytosine in 1 µg of tumor DNA was converted into uracil by bisulfite treatment with the EZ-96 DNA Methylation Kit (Zymo Research Corporation; www.zymoresearch.com) according to the manufacturer's instructions. PCR reactions were carried out in duplicate with each of the two selected primer pairs, for a total of four replicates per sample. For each replicate, 1 ml of bisulfite-treated DNA was used as template for a 5-ml PCR reaction in a 384-well microtiter plate, using 0.2 units of KAPA2G Fast HotStart DNA Polymerase (Kapa Biosystems; www.kapabiosystems.com), 200 mM dNTPs and 400 nM of each primer. Cycling conditions were: 94°C for 15 minutes; 45 cycles of 94°C for 20 seconds, 56°C for 30 seconds, 72°C for 1 minute; and one final cycle at 72°C for 3 minutes. Unincorporated dNTPs were deactivated using 0.3 U of shrimp alkaline phosphatase (SAP) in 2 ml, at 37°C for 20 minutes, followed by heat inactivation at 85°C for 5 minutes. Two ml of SAP-treated reaction were transferred into a fresh 384-well microtiter plate, and *in vitro* transcription and T cleavage were carried out in a single 5-ml reaction mix, using the MassCLEAVE kit (Sequenom) containing 1x T7 polymerase buffer, 3 mM dithiothreitol (DTT), 0.24 ml of T Cleavage mix, 22 U T7 RNA and DNA polymerase and 0.09 mg/ml RNAse A. The

reaction was incubated at 37°C for 3 hours. After the addition of a cation exchange resin to remove residual salt from the reactions, 10 nl of EpiTYPER reaction product was loaded onto a 384-element SpectroCHIP II array (Sequenom). SpectroCHIPs were analyzed using a Bruker Biflex III MALDI-TOF mass spectrometer (SpectroREADER, Sequenom). Results were analyzed using the EpiTYPER Analyzer software and manually inspected for spectra quality and peak quantification. *In vitro* treatment with 5-aza-2'-deoxycytidine was as described (Mavrakis, et al. 2008).

HELP (HpaII tiny fragment enrichment by ligation-mediated PCR) Assay for DNA Methylation

DLBCL specimens were obtained from patients at the BC Cancer Agency in Vancouver or at Weill Cornell Medical Center. The use of human tissue was in agreement with research ethics boards of the Vancouver Cancer Center/University of British Columbia and Weill Cornell Medical Center. The HELP assay was performed as previously published (Shaknovich, Figueroa and Melnick 2010) using two probes located upstream of, and overlapping with, the transcriptional start site of the *EPHA7* gene. Products of HELP were hybridized to human HG17 custom promoter arrays (Roche NimbleGen, Inc.; www.nimblegen.com) covering 25,626 HpaII amplifiable fragments. Data quality control and analysis were performed as described (Thompson, et al. 2008). After quality control processing, a quintile normalization was performed on each array. DNA samples profiled by HELP were also subjected to bisulfite treatment and MassARRAY EpiTYPER analysis as previously described. In order to cover all possible sites of digestion, primers were designed to cover the outermost HpaII sites of the selected HpaII amplifiable fragments (HAF) as well as any other HpaII sites up to 2,000 base pairs upstream or downstream of the HAF. Correlation of MassARRAY results with normalized data from HELP assay revealed a Spearman's rank correlation of R=0.88. The adjusted linear regression model was used to obtain the conversion formula.

Immunohistochemical and Tissue Microarray (TMA) Methods

The study cohort for analysis of EphA7 expression comprised FLs consecutively ascertained at the Memorial Sloan-Kettering Cancer Center (MSKCC) between 1985 and 2000. All cancer

biopsies were evaluated at MSKCC, and the histological diagnosis was based on hematoxylin and eosin (H&E) staining. Use of tissue samples was approved by MSKCC's Institutional Review Board and Human Biospecimen Utilization Committee. TMAs were constructed as previously described (Scott, et al. 2007) except that a fully automated arrayer (Beecher Instruments ATA-27) was used. TMAs were pre-treated with Cell Conditioning Solution 1 (Ventana Medical Systems, Inc.; www.ventanamed.com), incubated with EphA7 rabbit polyclonal antibody from Abgent (www.abgent.com) at 1:50 dilution for 60 minutes and then stained with secondary anti-rabbit antibody from Vector Laboratories, Inc. (www.vectorlabs.com) at 1:200 dilution for 60 minutes. Cores were scored as 0, 1 or 2 where 0=no staining; 1 = focal, weak staining; and 2 = moderate-to-strong staining in more than 50% of tumor cells.

Antibody Production and Purification

To construct the anti-CD20-EphA7 antibody, we amplified the $EphA7^{ECD}$ coding sequence by PCR from human genomic DNA. The PCR product was cloned into pAH6747, which contains an IgG1 constant region with an anti-CD20 heavy chain variable region (Dr. Sherie Morrison, UCLA). For antibody production, the anti-CD20-EphA7 heavy chain construct derived from pAH6747 and an anti-CD20 light chain (pAG10818) construct (Dr. Sherie Morrison, UCLA) were co-transfected into 293T cells, and the media in which the cells were growing was replaced every other day. Anti-CD20-EphA7 was purified from this conditioned media via affinity chromatography using recombinant Protein A. Briefly, the harvested media containing anti-CD20-EphA7 was dialyzed into 20 mM sodium phosphate (pH 7), passed over a 1 ml HiTrap rProtein A FF column (GE Healthcare Life Sciences; www.gelifesciences.com) and eluted with 100 mM glycine-HCl (pH 2.7). Eluant was collected in glass fraction tubes and immediately neutralized with 75 µl 1M Tris-HCl (pH 9.0) per ml of eluant. The antibody-containing peak fractions were pooled, dialyzed into phosphate-buffered saline and sterile filtered. Purity was determined by sodium dodecyl sulfate-polyacrylamide gel electrophoresis (SDS-PAGE), and antibody-fusion product concentration was determined with a spectrophotometer (280 nm) using an extinction coefficient of 1.43. ELISA using anti-human IgG (H+L) (Jackson ImmunoResearch Laboratories, Inc.; www.jacksonimmuno.com; #709-005-149) and horseradish peroxidase-conjugated-anti-

human IgG Fc (Jackson ImmunoResearch Laboratories, Inc.; #709-035-098) antibodies was used to verify protein purity and integrity.

Cell Culture, Cell Viability and Proliferation Assays, Vectors and Pooled shRNA Library Screen

FL5-12 murine lymphocytes were stably transduced with *BCL2* (FL5-12/*BCL2*); IL-3 depletion studies and viral transductions were as described (Mavrakis, et al. 2008). Cell viability was assessed using the Guava Viacount Assay (Millipore Corporation; www.millipore.com and LDS751 cell-permeant nucleic acid stain (Invitrogen; www.invitrogen.com) as previously described (Mavrakis, et al. 2008). The retroviral constructs utilized are based on MSCV and include *BCL2* (Wendel, et al. 2004) and individual or pooled shRNA constructs (Dickins, et al. 2005). Pooled shRNA screening technology has been described (Mavrakis, et al. 2010). Briefly, the shRNA library was constructed by pooling the individually cloned shRNAs. The screen design is depicted in Figure 4a. FL5-12/*BCL2* cells were transduced at low multiplicity of infection with the library pool containing 262 shRNAs and subjected to 7 days of IL-3 depletion. After recovery of viability, samples were collected for DNA isolation. Integrated shRNAs were amplified by PCR, subcloned into the pGEM-T Easy Vector (Promega) and identified by shRNA sequencing. Individual 'hits' from the screen were re-tested in the same *in vitro* assay and confirmed using multiple shRNAs against the same genes. The shRNAs against *PTEN* and *p53* have been previously reported (Mavrakis, et al. 2010) (Wendel, et al. 2006).

Generation, Treatment and Analysis of Tumors in Mice

The vavP-*BCL2* model of FL (Egle, et al. 2004) and the adoptive transfer of retrovirally transduced HPCs (Wendel, et al. 2004) have been described. Data were analyzed in Kaplan-Meier format using the log-rank (Mantel-Cox) test for statistical significance. H&E staining, terminal deoxynucleotidyl transferase dUTP nick end labeling (TUNEL) and analyses for Ki67, cleaved caspase, B220 and other surface markers were as described by Mavrakis, et al. (2008). Tumor xenografts were established by subcutaneous injection of 1 x 10^6 Raji or SU-DHL-10 human lymphoma cells mixed with Matrigel (BD Biosciences; www.bdbiosciences.com) into the flanks of NOD/SCID (NOD.CB17-Prkdc(scid)/J) mice. Once tumors exceeded 1 cm^3 in size, mice

were treated by three intratumoral injections of vehicle or 20 µg EphA7^{FC} (Recombinant Mouse EphA7 Fc Chimera; R&D Systems; www.rndsystems.com). Tumors were weighed and volumes were measured as described (Bergers, et al. 1999). Systemic administration of EphA7^{FC} and anti-CD20-EphA7 was by tail vein injection.

Western Blot Analysis, ELISA, and Protein Arrays

Immunoblots were performed from whole cell lysates or supernatant as described (Wendel, et al. 2004). Briefly, 50 µg of protein per sample were resolved on SDS-PAGE gels, transferred to Immobilon-P Transfer Membranes (Millipore) and probed with antibodies against EphA7 (Santa Cruz Biotechnology, Inc.; www.scbt.com; #sc-917 diluted 1:200), EphA2 (Millipore, Inc. #05-480 diluted 1:1000), Bcl2 (Santa Cruz Biotechnology, Inc. #sc-509 diluted 1:500), c-Myc (Santa Cruz Biotechnology, Inc. #sc-40 diluted 1:200), phosphorylated eIF4E-BP1 (Cell Signaling Technology, Inc.; www.cellsignal.com ; #9451 diluted 1:1000), phosphorylated Erk1/2 (Cell Signaling Technology, Inc. #9101 diluted 1:800), Erk1/2 (Cell Signaling Technology, Inc. #9102 diluted:1000), phosphorylated Src (Cell Signaling Technology, Inc. #2101 diluted 1:1000), phosphorylated S6 ribosomal protein (Cell Signaling Technology, Inc. # 2215 diluted 1:1000), phosphorylated Akt (Cell Signaling Technology, Inc. #4058 diluted 1:1000) and tubulin (Sigma-Aldrich Co.; www.sigmaaldrich.com; #T5168 diluted 1:5000). Blots were developed chemiluminescently using the Amersham ECL Western Blotting System (GE Healthcare Life Sciences). ELISA for phosphorylated EphA2 in Raji cell lysates was performed utilizing the Human Phospho-EphA2 DuoSet IC (R&D Systems #DYC4056-2) according to the manufacturer's instructions. A human phosphoprotein detection array (R&D Systems #ARY003) was probed with cell lysates according to the manufacturer's instructions.

Production of EphA7^{Fc} Protein

In addition to the EphA7^{Fc} protein obtained from commercial sources (R&D Systems; see above), we produced an identical protein using a baculoviral expression system. A DNA fragment corresponding to EphA7 amino acids Lys31 through Asn525 was cloned into the BamH1/Not1 sites of the pAcGP67B-based (BD Biosciences) pMA152, a baculovirus vector with

an IgG Fc-tag at the C-terminus of the protein-coding region (Antipenko, et al. 2003) (Xu, et al. 2008). The recombinant baculovirus constructs were co-transfected, with BaculoGold linearized baculovirus DNA (BD Biosciences), into Sf9 insect cells. Passage four recombinant baculovirus was used to infect Hi-5 cells in suspension at a density of 1.8 x 10^6 cells/ml in Sf-900 II SFM protein-free insect cell culture medium (Invitrogen). Infected cells were grown at 27°C and 100 rpm and harvested after 64 hours. Hi-5 cell supernatant containing the secreted $EphA7^{Fc}$ was loaded onto a Protein A Sepharose column and eluted by a step-wise pH gradient fractionation in 100 mM glycine. The yield was 1-2 mg protein per liter of Hi-5 cell suspension (Antipenko, et al. 2003) (Xu, et al. 2008).

qRT-PCR

Total RNA was extracted from tumor samples and cell lines using the AllPrep DNA/RNA/Protein Mini Kit (Qiagen). cDNA synthesis, real-time-PCR and analysis by the ΔΔ Ct method were performed as described (Mavrakis, et al. 2008). EphA7 PCR utilized TTTCAAACTCGGTACCCTTCA as forward primer and CATTGGGTGGAGAGGAAATC as reverse primer and SYBR green detection; glyceraldehyde 3-phosphate dehydrogenase (gapdh) was used as a standard (GAGTCAACGGATTTGGTCGT forward primer, GACAAGCTTCCCGTTCTCAG reverse primer and SYBR green detection); and human beta glucuronidase (gusb; Applied Biosystems; www.appliedbiosystems.com; #4333767F) was used as an endogenous control.

PCR Amplification and Sequencing of Genomic DNA

Sequencing of genomic DNA was performed as described (Veeriah, et al. 2010). Genomic DNA was amplified using a REPLI-g Midi Kit (Qiagen). The exonic regions of interest (NCBI Build 36.1) were broken into amplicons of 500 bp or less, and the Primer3 program was used to design specific primers covering exonic regions plus at least 50 base pairs of flanking intronic sequence. M13 tails were added to facilitate Sanger sequencing. PCR reactions were carried out in 384-well plates in a Duncan DT-24 (KBiosystems Limited; www.kbiosystems.com) water bath thermal cycler, with 10 ng of amplified DNA as template, using a touchdown PCR protocol with Taq HotStart DNA Polymerase (Kapa Biosystems). The touchdown cycling conditions were:

95°C for 5 minutes; three cycles of 95°C for 30 seconds, 64°C for 30 seconds, 72°C for 60 seconds; three cycles of 95°C for 30 seconds, 62°C for 30 seconds, 72°C for 60 sec; three cycles of 95°C for 30 sec, 60°C for 30 seconds, 72°C for 60 seconds; 37 cycles of 95°C for 30 seconds, 58°C for 30 seconds, 72°C for 60 seconds; and one final cycle at 70°C for 5 minutes. The resulting DNA sequencing templates were purified using Agencourt AMPure (Beckman Coulter, Inc.; www.beckmangenomics.com). The purified PCR reaction products were split in two, and sequenced bidirectionally with M13 forward and reverse primers and BigDye Terminator v3.1 Cycle Sequencing kit (Applied Biosystems). Dye terminators were removed using the Agencourt CleanSEQ kit (Beckman Coulter, Inc.), and sequence reactions were run on an ABI PRISM 3730xl sequencing apparatus (Applied Biosystems).

Mutation Detection

Mutations were detected using an automated detection pipeline at the MSKCC Bioinformatics Core. Bi-directional sequencing reads and mapping tables (to link read names to sample identifiers, gene names, read direction and amplicon) were subjected to a filter that excludes reads that have an average Phred score of <10 for bases 100-200. Passing reads were assembled against the reference sequences for each gene, containing all coding and untranslated exons including 5 kb upstream and downstream of the gene, using command line Consed 16.0 (Gordon, Abajian and Green 1998). Assemblies were passed on to PolyPhred 6.02b (Nickerson, Tobe and Taylor 1997), which generated a list of putative candidate mutations, and to PolyScan 3.0 (Chen, et al. 2007), which generated a second list of putative mutations. The lists were merged together into a combined report, and the putative mutation calls were normalized to '+' genomic coordinates and annotated using the Genomic Mutation Consequence Calculator. The resulting list of annotated putative mutations was loaded into a PostgreSQL database along with select assembly details for each mutation call (assembly position, coverage and methods supporting mutation call). To reduce the number of false positives generated by the mutation detection software packages, only point mutations supported by at least one bi-directional read pair and at least one sample mutation called by PolyPhred were considered, and only putative mutations that are annotated as having

nonsynonymous coding effects, occur within an exon or within 11 base pairs of an exon boundary, or have a conservation score >0.699 were included in the final candidate list. Indels called by any method were manually reviewed and included in the candidate list if found to hit an exon. All putative mutations were confirmed by a second PCR and sequencing reaction, in parallel with amplification and sequencing of matched normal tissue DNA. All traces for mutation calls were manually reviewed.

DESCRIPTION OF FIGURES

Figure 1. Oncogenomic study to identify tumor suppressor genes in FL. a. The study design combines genomic tumor analyses with an RNAi screen and validation in murine models and in xenografts; **b.** aCGH analysis of 68 FLs showing frequencies of genomic gain (red) and loss (blue) across the genome; **c.** High resolution depiction of recurrent gains (red) and losses (blue) affecting chromosome 6q with CRDs indicated; **d.** Mapping of CRDs. The observed 6q deletions are typically large and hemizygous and do not readily identify a target gene.

Figure 2. Case-by-case analysis of gains and losses across chromosome 6q in FLs. a. Regions of copy number loss and gain aligned with a map of chromosome 6. Losses are indicated in blue and gains in red with color intensity representing the signal strength. Location of some key genes as well as of CRD4 and CRD9 is indicated. **b.** *EPHA7* is affected in eight of 13 deletions involving CRD4; similarly *TNFAIP3* is affected in nine of twelve cases harboring CRD9 deletions. **c.** *EPHA7*, *PRDM1* and *TNFAIP3* are frequently co-deleted. Among 64 FL cases, deletions affect *EPHA7* in eight (12.5%), *PRDM1* in six (9.4%) and *TNFAIP3* in nine (14%). In five of 64 FLs (7.8%), all three genes are affected. The deletions are almost entirely hemizygous, and no gene is directly affected by bi-allelic loss. The size of the deletions and the complex pattern suggest multiple targets; however the genomic data alone do not pinpoint any specific gene associated with FL.

Figure 3. aCGH analysis of six HIV-associated BLs. a. Segmental analyses corrected for CNVs reveals 6q deletions in two of six cases compared to a reference. **b.** Whole genome changes and the proportion of BLs affected. The smallest common region of deletion in 6q is extends from nucleotide 84,341,552 through nucleotide 117,084,517, which overlaps with CRDs 4-7 in FLs and includes *EPHA7* and *PRDM1*.

Figure 4. RNAi screen and *in vivo* validation of candidate tumor suppressor genes. a. Design of a pooled, deletion-specific shRNA library screen in a surrogate model (immortalized FL5-12/*BCL2* cells). **b.** Fluorescence-activated cell sorting (FACS) analyses of cells transduced with the pooled 6q deletion library showing enrichment of cells expressing shRNAs (and the GFP reporter) following IL-3 depletion. **c.** Absolute number and identity of shRNA sequences retrieved from the enriched population. **d.** *EPHA7* and *TNFAIP3* map, respectively, to the CRD4 and CRD9 in FL; *PRDM1* did not score in this screen. **e.** Adoptive transfer enables genetic studies in the vavP-*BCL2* model of FL. **f.** Tumor latencies for animals receiving vavP-*BCL2* transgenic HPCs transduced with empty vector (black, n = 11), or shRNAs against *EPHA7* (red, n = 18) or *p53* (green, n = 9) or over-expressing *c-MYC* (blue, n = 7). **g.** Microscopic pathology and immunohistochemistry of vavP-*BCL2* lymphomas expressing the indicated constructs. Red arrows indicate infiltrating tumor cells.

Figure 5. Individual validation of the screen results. FL5-12/*BCL2* cells partially transduced with indicated shRNA/GFP or control constructs are shifted into IL-3-deficient media and monitored for changes in the proportion of GFP-expressing cells. An increase in the proportion of GFP-expressing cells (indicated with red outline) implicates co-transduced genes in the survival and proliferation of Bcl2-expressing B-cells upon IL-3 depletion.

Figure 6. Characterization of *EPHA7* shRNAs. a. Assessment of three shRNAs (sh1-3) targeting *EPHA7* in FL5-12/*BCL2* cells as described in Figure 5. **b**. Lysates of FACS-sorted FL5-12/*BCL2* cells expressing one of three shRNAs targeting *EPHA7* (sh1-3) or vector (V) blotted and probed with antibodies as indicated. (p21 has been reported as a common off-target of shRNAs.)

Figure 7. Role of *TNFAIP3* in vavP-*BCL2* HPC recipient animals. **a.** Tumor latencies for animals receiving vavP-*BCL2* transgenic HPCs transduced with empty vector (black, n = 11), or shRNAs targeting *EPHA7* (red, n = 18), *TNFAIP3* (green, n = 3) or *EPHA7* and *TNFAIP3* (blue, n = 5). **b.** Lysates of FL5-12/*BCL2* cells expressing vector or an shRNA targeting TNFAIP3 blotted and probed with antibodies as indicated.

Figure 8. Microscopic pathology and immunohistochemistry of vavP-*BCL2* lymphomas. Red arrows indicate infiltrating tumor cells.

Figure 9. Molecular characterization of murine vavP-*BCL2* lymphomas. **a.** Location of primers used to analyze clonality. **b.** Nested PCR analysis of DJ recombination reveals a single band at ~140bp, indicating clonality of this vavP-*BCL2/EPHA7* lymphoma. **c.** PCR analysis of DJ recombination in lymphomas arising in transgenic vavP-*BCL2* animals and in mice receiving HPCs transduced with the indicated shRNA constructs confirms their clonality. **d.** Lysates from vavP-*BCL2* transgenic HPCs (HSC) and splenocytes (spleen) blotted and probed with antibodies as indicated. **e.** Whole tumor lysates of vavP-*BCL2* tumors expressing *c-MYC* or shRNAs targeting *EPHA7*, *FOXO3* or *p53*and probed with antibodies as indicated.

Figure 10. Candidate tumor suppressor genes in the Eμ-*MYC* lymphoma model. **a**. Diagram comparing the 6q deletions seen in FL and BL. **b.** the Eμ-*MYC* model and our HPC transplantation approach. **c**. Tumor latencies for animals receiving Eμ-*MYC* transgenic HPCs transduced with empty vector (black, n = 60, including concurrent and historic controls), with shRNA against *EPHA7* (red, n = 11) or with *AKT* (blue, n = 8); $p_{(sh\mathit{EPHA7}\text{ or }\mathit{AKT}\text{ vs. vector})} < 0.05$. **d.** Lysates from vector- or sh*EPHA7*-expressing Eμ-*MYC* lymphomas blotted and probed as indicated. **e**. Microscopic pathology and immunohistochemistry of Eμ-*MYC* lymphomas expressing the indicated constructs.

Figure 11. *EPHA7* is differentially silenced in FLs and expressed in GC B-cells. a. qRT-PCR results for *EPHA7* in purified B-cells from reactive tonsils (T), GC, FLs and BLs. Results are displayed as mean ± standard deviation; $p_{(tumor\ vs.\ normal)} < 0.05$ for FL and BL. **b.** Immunohistochemical detection of the EphA7 protein in a normal tonsil. **c.** Representative section of TMA representing 322 human FLs stained for EphA7. **d and e.** MassARRAY analysis of *EPHA7* promoter methylation in 32 FLs **(d)** and 16 human lymphoma lines **(e)** and positive/negative controls (Ctrl); the color scale indicates the degree of methylation with red indicating 0% and yellow 100%. **f.** qRT-PCR of *EPHA7* mRNA levels in human lymphoma cell lines treated with 5-aza-2'-deoxycytidine (Aza); $p_{(Aza\ vs.\ untreated)} < 0.01$ for all cell lines; Raji cells are hemizygous for *EPHA7*.

Figure 12. Higher resolution EphA7 immunohistochemistry of human tissues. a. EphA7 stain of normal tonsil. **b and c.** Representative negative **(b)** and positive **(c)** stains of human FLs on the TMA. (The TMA also includes, as controls, normal human kidney and liver and gastric cancers with known EphA7 staining patterns.)

Figure 13. HELP analysis of differential *EPHA7* promoter methylation in normal GC B-cells, FL, DLBCL and DLBCL-derived cell lines. a. Location of the probes used to analyze *EPHA7* promoter methylation. **b and c.** Results with probe 1 comparing centroblasts (CB; n = 9) with FL (n = 8) and DLBCL (n = 155) **(b)** and CB with DLBCL-derived cell lines **(c)**. **d and e.** Analogous results for probe 2. Silencing is progressive from GC B-cells to FL and aggressive DLBCL and nearly complete in DLBCL lines (* indicates $p < 0.05$). The data are consistent with MassARRAY and expression data and indicate differential silencing between lymphomas and GC B-cells.

Figure 14. Characterization of $EphA7^{ECD}$ expressed from a 5-aza-2'-deoxycytidine-treated human lymphoma line. a. RT-PCR showing re-expression of the *EPHA7* transcript in SU-DHL-10 cells upon treatment with 1 µg and 5 µg 5-aza-2'-deoxycytidine (Aza). **b.** cDNA sequence (SEQ ID NO: 01) of the re-expressed RNA. **c.** Translation (SEQ ID NO: 02) of the cDNA sequence (SEQ ID NO: 01). **d.** Domain structure of the protein encoded by the re-expressed RNA. **e.** Predicted three-dimensional structure based on similarity with the known EphA2 structure. **f.** Gel purification of the Fc-tagged ectodomain of EphA7 ($EphA7^{Fc}$).

Figure 15. Analysis of the *EPHA7* locus and its expression in Raji lymphoma cells. a. Genomic qPCR to determine *EPHA7* gene copy number in Raji lymphoma cells is consistent with loss of one allele of *EPHA7* in these cells. **b.** qRT-PCR of *EPHA7* mRNA confirms the absence of *EPHA7* expression in Raji cells compared to normal tonsils (* denotes $p < 0.05$).

Figure 16. EphA7^{Fc} can block oncogenic signals and suppress the growth of xenografted human lymphomas. a. Lysates and conditioned media from FL5-12/*BCL2* cells expressing empty vector, an shRNA targeting *EPHA7* (shEphA7) or full length *EPHA7* (EphA7FL) probed with an antibody against EphA7. **b.** Immunoprecipitation of lysates of Raji cells treated with EphA7^{Fc} (Fc-tagged ectodomain of EphA7) or with Fc control, immunoprecipitated with anti-EphA7 antibody and probed with antibodies to EphA7 or EphA2. **c.** ELISA for EphA2 phosphorylation in Raji cells treated with Eph7^{Fc} or Fc. **d.** Immunoblot of lysates of Raji cells treated with Fc control, EphA7^{Fc} (5 μg) or a small interfering RNA (siRNA) directed against EphA2. **e.** Immunoblot of lysates of Raji cells treated with 5μg/ml EphA7^{Fc} as indicated. **f.** Model of the EphA2 – EphA7^{ECD} interaction based on the known structure of EphA2 and its homology with EphA7 (LBD, ligand binding domain; EGF, EGF-like domain; FNIII, fibronectin domain). **g.** Xenografted Raji lymphomas grown in the flanks of NOD/SCID mice and treated three times on alternate days by intratumoral administration of 20 μg EphA7^{Fc} (red circle) or vehicle (Fc; black circle). **h.** Microscopic pathology of EphA7^{Fc}-treated and mock-treated Raji lymphomas stained as indicated. **i.** Immunoblot of lysates of tumors treated with EphA7^{Fc} or vehicle (Fc) *in vivo*. **j.** Matched-pair analysis of tumor volumes of eight (A-H) EphA7^{Fc}-treated (red) and vehicle (Fc)-treated (black) Raji lymphomas. **k.** Intravenous (i.v.) administration of EphA7^{Fc} (20μg/day x3 days; red) delays tumor development following injection of 1×10^6 Raji lymphoma cells vs. administration of vehicle (Fc). **l.** Schematic of anti-CD20-EphA7 antibody. **m.** Immunoblot of lysates of Raji cells treated with anti-CD20 antibody (CD20), with anti-CD20-EphA7 antibody (CD20/E7) or untreated (Untr.). **n.** Proliferation of Raji cells treated as indicated; * denotes $p_{(CD20/E7 \text{ vs. } CD20)} < 0.05$. **o.** Apoptosis of Raji cells treated as indicated at 24 hours and 48 hours (* and ** denote $p < 0.05$). **p.** Weight of tumors from mice bearing Raji xenografts (>1cm^3) left untreated (Untr.) or given 1 μg/day x 5 days of anti-CD20 antibody (CD20) or anti-CD20-EphA7 antibody (CD20/E7). Tumors (in Matrigel) were collected two days after last treatment,

weighed *ex vivo* and classified as complete response (CR; 0 – 30 mg), partial responses (PR; 30-100 mg) or no change/progressive disease (NC/PD; >100 mg).

Figure 17. EphA7 signaling effects in human lymphoma cell lines. a. Immunoblot of lysates of DoHH2 cells treated with $EphA7^{Fc}$ or Fc, immunoprecipitated with anti-EphA7 antibody and probed with antibodies to EphA7 or EphA2. **b.** Confirmation of EphA2 expression in Raji cells by immunoblot. **c.** Immunoblot of lysates of Raji cells treated with an siRNA against EphA2 for the indicated times and probed as indicated. **d.** Immunoblot of cell lysates of SU-DHL-6, DoHH2, and Karpas 422 cells treated with $EPph7^{Fc}$ as indicated reveals some cell type-specific differences and similarities in signaling.

Figure 18. Signaling effects of $EphA7^{Fc}$ and shRNA-mediated *EPHA7* knockdown. a. FL5-12/*BCL2* cells expressing empty vector or shEphA7 probed with the indicated antibodies. **b.** FL5-12/*BCL2* cells expressing shEphA7 (FL5-12/*BCL2*/shEphA7) treated with $EphA7^{Fc}$ (5 µg/ml) for the indicated times and probed as indicated.

Figure 19. $EphA7^{Fc}$ affects several signaling molecules in human lymphoma cells. a. Phosphoprotein array probed with lysates from Raji cells treated for 15 minutes with 5 µg/ml purified $EphA7^{Fc}$ or vehicle. **b.** Quantification of phosphoprotein array results; the blue line indicates values for untreated cells. **c.** Dose-response relationship for $EphA7^{Fc}$-mediated Erk inhibition. **d and e.** Immunoblots of lysates of Raji (d) and SU-DHL-10 (e) lymphoma cells treated for 15 minutes with 5 µg/ml purified $EphA7^{Fc}$ or vehicle (v) and probed for the indicated signaling molecules.

Figure 20. Retroviral expression of $EPHA7^{ECD}$ in human lymphoma cells. a. qRT-PCR showing the level of retroviral expression of $EPHA7^{ECD}$ ($EPHA7^{TR}$) mRNA in Raji and SU-DHL-10 cells. **b.** Growth curve of FACS-sorted populations of vector- or $EPHA7^{ECD}$ ($EPHA7^{TR}$)-expressing Raji and SU-DHL-10 cells. **c.** Progressive depletion of $EPHA7^{ECD}$ ($EPHA7^{TR}$)/GFP-expressing Raji cells from mixed populations during 72 hours in *in vitro* culture.

Figure 21. Induction of apoptosis by EphA7^{Fc} in FL-derived cell lines *in vitro*. **a.** FACS analysis of apoptosis induced by treatment with 5 μg EphA7Fc in Raji, Karpas 422 and DoHH2 cells. **b.** Quantification of apoptosis in a panel of lymphoma lines (V, Vehicle/Fc; E7, EphA7^{Fc}; $p_{(E7 \text{ vs. } V)}$ <0.05).

Figure 22. Matched-pair analysis of xenografted SU-DHL-10 and Raji human lymphoma cells treated with EphA7^{Fc} or Fc. **a.** Photograph of tumors *ex situ* following treatment with 20μg EphA7^{Fc} or Fc (vehicle). **b.** Tumor weights comparing EphA7^{Fc}-treated and Fc-treated tumors ($p < 0.05$ for SU-DHL-10 and Raji).

Figure 23. Purification and functional characterization of an anti-CD20-EphA7^{ECD} fusion antibody. **a.** ELISA measurement of anti-CD20 and anti-CD20-EphA7antibody production. **b.** FACS analysis of CD20^{+} Raji cells treated with the anti-CD20 or anti-CD20-EphA7 antibodies and a fluorescein isothiocyanate (FITC)-labeled anti-IgG antibody. **c.** ELISA of EphA2 phosphorylation in Raji cells treated with Fc (Untr.), EphA7^{Fc} or anti-CD20-EphA7 (* indicates $p_{(\text{either treatment vs. vehicle})} < 0.05$).

Figure 24. Anti-CD20-EphA7 induces cell death and blocks proliferation of DoHH2 lymphoma cells. **a.** Apoptosis of untreated (Untr.), anti-CD20 (CD20)- or anti- CD20-EphA7 (CD20/E7)-treated DoHH2 cells at 24 hours and 48 hours. **b.** Proliferation of DoHH2 cells untreated (Untr.), treated with anti-CD20 (CD20) or anti-CD2-EphA7 antibody (CD20/E7).

Figure 25. Microscopic histology and immunohistochemistry of Raji xenografts. Tumors were treated with anti-CD20-EphA7 antibody (1μg/day x 5 days) or vehicle and collected two hours after the final treatment. The anti-CD20-EphA7-treated tumors reveal some increase in TUNEL positivity, reduced proliferation and reduced Erk phosphorylation.

REFERENCES

Adams, J. M., et al. "The c-myc Oncogene Driven by Immunoglobulin Enhancers Induces Lymphoid Malignancy in Transgenic Mice." *Nature* 318, no. 6046 (December 1985): 533-538.

Antipenko, Alexander, et al. "Structure of the Semaphorin-3A Receptor Binding Module." *Neuron* 39, no. 4 (August 2003): 589-598.

Bende, R J, L A Smit, and C J van Noesel. "Molecular Pathways in Follicular Lymphoma." *Leukemia* 21, no. 1 (January 2007): 18-29.

Bergers, Gabriele, Kashi Javaherian, Kin-Ming Lo, Judah Folkman, and Douglas Hanahan. "Effects of Angiogenesis Inhibitors on Multistage Carcinogenesis in Mice." *Science* 284, no. 5415 (April 1999): 808-812.

Chen, Ken, et al. "PolyScan: An Automatic Indel and SNP Detection Approach to the Analysis of Human Resequencing Data." *Genome Research* 17, no. 5 (May 2007): 659-656.

Compagno, Mara, et al. "Mutations of Multiple Genes Cause Deregulation of NF-κB in Diffuse Large B-cell Lymphoma." *Nature* 459, no. 7247 (June 2009): 717-721.

Dawson, D. W., et al. "Global DNA Methylation Profiling Reveals Silencing of a Secreted Form of Epha7 in mouse and human germinal center B-cell lymphomas." *Oncogene* 26, no. 29 (June 2007): 4243-4252.

Egle, Alexander, Alan W. Harris, Mary L. Bath, Lorraine O'Reilly, and Suzanne Cory. "VavP-Bcl2 Transgenic Mice Develop Follicular Lymphoma Preceded By Germinal Center Hyperplasia." *Blood* 103, no. 6 (March 2004): 2276-2283.

Gaidano, Gianluca, et al. "Deletions Involving Two Distinct Regions of 6q in B-Cell Non-Hodgkin Lymphoma." *Blood* 80, no. 7 (October 1992): 1781-1787.

Gordon, David, Chris Abajian, and Phil Green. "Consed: A Graphical Tool for Sequence Finishing." *Genome Research* 8, no. 3 (March 1998): 195-202.

Hauptschein, Robert S., et al. "Cloning and Mapping of Human Chromosome 6q26–q27 Deleted in B-Cell Non-Hodgkin Lymphoma and Multiple Tumor Types." *Genomics* 50, no. 2 (June 1998): 170-186.

Himanen, Juha P., et al. "Architecture of Eph Receptor Clusters." *Proceedings of the National Academy of Sciences of the United State of America* 107, no. 24 (June 2010): 10860-10865.

Holmberg, Johan, Diana L. Clarke, and Jonas Frisén. "Regulation of Repulsion versus Adhesion by Different Splice Forms of an Eph Receptor." *Nature* 408, no. 6809 (November 2000): 203-206.

Johnson, Nathalie A., et al. "Lymphomas with Concurrent BCL2 and MYC Translocations: The Critical Factors Associated with Survival." *Blood* 114, no. 11 (September 2009): 2273-2279.

Kuang, Shao-Qing, et al. "Aberrant DNA Methylation and Epigenetic Inactivation of Eph Receptor Tyrosine Kinases and Ephrin Ligands in Acute Lymphoblastic Leukemia." *Blood* 115, no. 12 (March 2010): 2412-2419.

Mandelbaum, Jonathan, et al. "BLIMP1 Is a Tumor Suppressor Gene Frequently Disrupted in Activated B Cell-like Diffuse Large B Cell Lymphoma." *Cancer Cell* 18, no. 6 (December 2010): 568-579.

Mavrakis, K. J., et al. "Tumorigenic Activity and Therapeutic Inhibition of Rheb GTPase." *Genes & Development* 22, no. 16 (August 2008): 2178-2188.

Mavrakis, Konstantinos J, et al. "Genome-wide RNA-mediated Interference Screen Identifies miR-19 Targets in Notch-induced T-cell Acute Lymphoblastic Leukaemia." *Nature Cell Biology* 12, no. 4 (April 2010): 372-379.

McBride, Kevin M., Anna Gazumyan, Eileen M. Woo, Tanja A. Schwickert, Brian T. Chait, and Michel C. Nussenzweig. "Regulation of Class Switch Recombination and Somatic Mutation by AID Phosphorylation." *The Journal of Experimental Medicine* 205, no. 11 (October 2008): 2585-2594.

McCaffrey, Anton P., Leonard Meuse, Thu-Thao T. Pham, Douglas S. Conklin, Gregory J. Hannon, and Mark A. Kay. "Gene Expression: RNA Interference in Adult Mice." *Nature* 418, no. 6893 (July 2002): 38-39.

Nanjangud, G., et al. "Molecular Cytogenetic Analysis of Follicular Lymphoma (FL) Provides Detailed Characterization of Chromosomal Instability Associated with the t(14;18)(q32;q21) Positive and Negative Subsets and Histologic Progression." *Cytogenetics and Genome Research* 118, no. 2-4 (November 2007): 337-344.

Nickerson, Deborah A., Vincent O. Tobe, and Scott L. Taylor. "PolyPhred: Automating the Detection and Genotyping of Single Nucleotide Substitutions Using Fluorescence-based Resequencing." *Nucleic Acids Research* 25, no. 14 (July 1997): 2745-2751.

Noren, Nicole K., Gabriele Foos, Craig A. Hauser, and Elena B. Pasquale. "The EphB4 Receptor Suppresses Breast Cancer Cell Tumorigenicity Through an Abl–Crk Pathway." *Nature Cell Biology* 8, no. 8 (August 2006): 815-825.

Offit, K., et al. "6q Deletions Define Distinct Clinico-Pathologic Subsets of Non-Hodgkin's Lymphoma." *Blood* 82, no. 7 (October 1993): 2157-2162.

Oricchio, Elisa, Andrew L. Wolfe, Jonathan H. Schatz, Konstantinos J. Mavrakis, and Hans-Guido Wendel. "Mouse Models of Cancer as Biological Filters for Complex Genomic Data." *Disease Models & Mechansims* 3, no. 11-12 (November - December 2010): 701-704.

Pasquale, Elena B. "Eph Receptors and Ephrins in Cancer: Bidirectional Signalling and Beyond." *Nature Reviews Cancer* 10, no. 3 (March 2010): 165-180.

Relander, Thomas, Nathalie A. Johnson, Pedro Farinha, Joseph M. Connors, Laurie H. Sehn, and Randy D. Gascoyne. "Prognostic Factors in Follicular Lymphoma." *Journal of Clinical Oncology* 28, no. 17 (June 2010): 2902-2913.

Scott, Clare L., et al. "Role of the Chromobox Protein CBX7 in Lymphomagenesis." *Proceedings of the National Academy of Sciences of the United States of America* 104, no. 13 (March 2007): 5389-5394.

Seiradake, Elena, Karl Harlos, Geoff Sutton, A. Radu Aricescu, and E. Yvonne Jones. "An Extracellular Steric Seeding Mechanism for Eph-Ephrin Signaling Platform Assembly." *Nature Structural & Molecular Biology* 17, no. 4 (April 2010): 398-402.

Shaknovich, Rita, Maria E. Figueroa, and Ari Melnick. "HELP (Hpall Tiny Fragment Enrichment by Ligation-Mediated PCR) Assay for DNA Methylation Profiling of Primary Normal and Malignant B Lymphocytes." *Methods in Molecular Biology* 632 (2010): 191-201.

Taylor, Barry S., et al. "Functional Copy-Number Alterations in Cancer." *PLoS One* 3, no. 9 (September 2008): e3179.

Thompson, Reid F., et al. "An Analytical Pipeline for Genomic Representations Used for Cytosine Methylation Studies." *Bioinformatics* 24, no. 9 (May 2008): 1161-1167.

Valenzuela, D. M., et al. "Identification of Full-length and Truncated Forms of Ehk-3, a Novel Member of the Eph Receptor Tyrosine Kinase Family." *Oncogene* 10, no. 8 (April 1995): 1573-1580.

Veeriah, Selvaraju, et al. "Somatic Mutations of the Parkinson's Disease–associated Gene PARK2 in Glioblastoma and Other Human Malignancies." *Nature Genetics* 42, no. 1 (January 2010): 77-82.

Wendel, H. G., et al. "Survival Signalling by Akt and eIF4E in Oncogenesis and Cancer Therapy." *Nature* 428, no. 6980 (March 2004): 332-337.

Wendel, Hans-Guido, et al. "Loss of p53 Impedes the Antileukemic Response to BCR-ABL Inhibition." *Proceedings of the National Academy of Sciences of the United States of America* 103, no. 19 (May 2006): 7444-7449.

Xu, Kai, Kanagalaghatta R. Rajashankar, Yee-Peng Chan, Juha P. Himanen, Christopher C. Broder, and Dimitar B. Nikolov. "Host Cell Recognition by the Henipaviruses: Crystal Structures of the Nipah G Attachment Glycoprotein and its Complex with Ephrin-B3." *Proceedings of the National Academy of Sciences of the United States of America* 105, no. 29 (July 2008): 9953-9958.

Yu, Duonan, and Andrei Thomas-Tikhonenko. "A Non-transgenic Mouse Model for B-cell Lymphoma: In vivo Infection of p53-null Bone Marrow Progenitors by a Myc Retrovirus Is Sufficient for Tumorigenesis." *Oncogene* 21, no. 12 (March 2002): 1922-1927.

WE CLAIM

1. A fusion protein comprising a recombinant immunoglobulin (Ig) heavy chain or portion thereof having an amino-terminal variable region (Fv) that specifically binds to CD20 antigen, wherein said Ig heavy chain or portion thereof is linked at its carboxy-terminus by a peptide bond to the amino-terminal amino acid of tumor suppressor protein $EphA7^{ECD}$.

2. The fusion protein of Claim 1, wherein said tumor suppressor protein $EphA7^{ECD}$ comprises SEQ ID NO: 02.

3. A recombinant expression vector comprising a nucleotide sequence encoding the fusion protein of Claim 1.

4. A method for reducing one or more symptoms of cancer comprising administering to a subject in need thereof a therapeutically effective amount of at least one of the fusion protein of Claim 1 and the expression vector of Claim 3.

5. The method of Claim 4, wherein said cancer is lymphoma.

6. The method of Claim 4, wherein said cancer comprises cancer cells that

a) express CD20 protein, and

b) comprise one or more of

i) deletion of ephrin receptor A7 (*EPHA7*) gene,

ii) reduced expression of EphA7 protein, and

iii) increased expression of EphA2 protein.

7. The method of Claim 6, wherein said cancer cells comprise B cells.

8. The method of Claim 7, wherein said cancer is lymphoma.

9. The method of Claim 4, wherein said subject is human.

10. A method for identifying cancer cells responsive to the method of Claim 4, comprising determining in said cancer cells the presence of a deletion of ephrin receptor A7 (*EPHA7*) gene, wherein detecting deletion of said *EPHA7* gene identifies said cancer cells as responsive to the method of Claim 4.

11. A method for identifying cancer cells responsive to the method of Claim 4, comprising determining expression of EphA7 protein by said cancer cells, wherein detecting reduced

expression of said EphA7 protein identifies said cancer cells as responsive to the method of Claim 4.

12. A method for identifying cancer cells responsive to the method of Claim 4, comprising determining expression of EphA2 protein by said cancer cells, wherein detecting increased expression of said EphA2 protein identifies said cancer cells as responsive to the method of Claim 4.

13. A fusion protein comprising a recombinant immunoglobulin (Ig) heavy chain or portion thereof having an amino-terminal variable region (Fv) that specifically binds to a tumor cell surface marker antigen, wherein said Ig heavy chain or portion thereof is linked at its carboxy-terminus by a peptide bond to the amino-terminal amino acid of tumor suppressor protein $EphA7^{ECD}$.

14. The fusion protein of Claim 13, wherein said tumor suppressor protein $EphA7^{ECD}$ comprises SEQ ID NO: 02.

15. A recombinant expression vector comprising a nucleotide sequence encoding the fusion protein of Claim 13.

16. A method for reducing one or more symptoms of cancer comprising administering to a subject in need thereof a therapeutically effective amount of at least one of the fusion protein of Claim 13 and the expression vector of Claim 15.

17. The method of Claim 16, wherein said cancer is lymphoma.

18. The method of Claim 16, wherein said cancer comprises cancer cells that

a) express CD20 protein, and

b) comprise one or more of

i) deletion of ephrin receptor A7 (*EPHA7*) gene,

ii) reduced expression of EphA7 protein, and

iii) increased expression of EphA2 protein.

19. The method of Claim 18, wherein said cancer cells comprise B cells.

20. The method of Claim 19, wherein said cancer is lymphoma.

21. The method of Claim 16, wherein said subject is human.

Application number / Numéro de demande: 2832184

Figures: 1A-D, 2A-C, 3a-3b, 4A-D, 5, 6A, 6B, 7A, 7B & 9A-E, 10A-D, 11A-F, 12A-C 13A-E, 14A-F, 15A, 15B, 16A-P, 17A-D 18A, 18B, 19A-E, 20A-C, 22A, 22B, 25

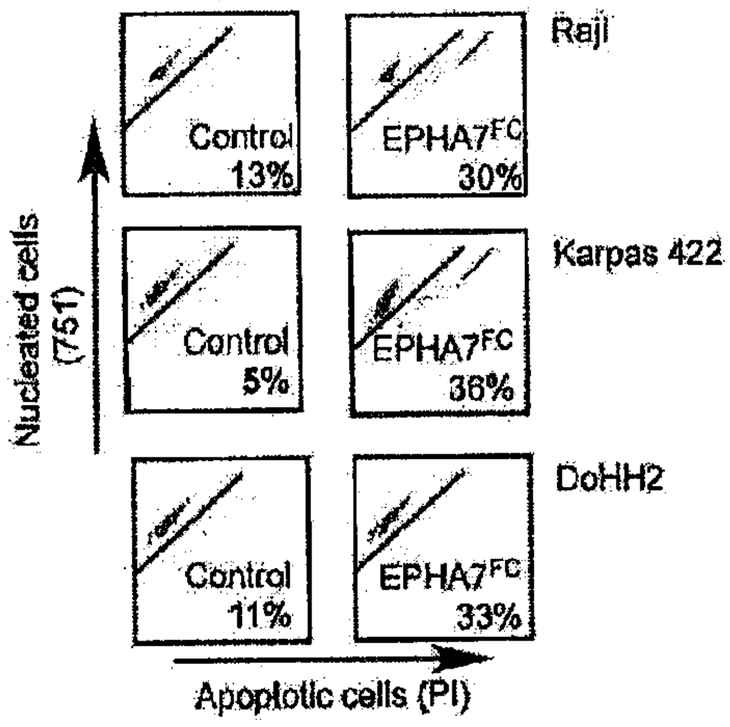
Pages:

Unscannable items received with this application
(Request original documents in File Prep. Section on the 10th floor)

Documents reçu avec cette demande ne pouvant être balayés
(Commander les documents originaux dans la section de la préparation des dossiers au 10ième étage)

Figure 21

a


Raji
Control
13%
EPHA7FC
30%
Karpas 422
Control
5%
EPHA7FC
36%
DoHH2
Control
11%
EPHA7FC
33%
Nucleated cells (7-AAD)
Apoptotic cells (PI)

b

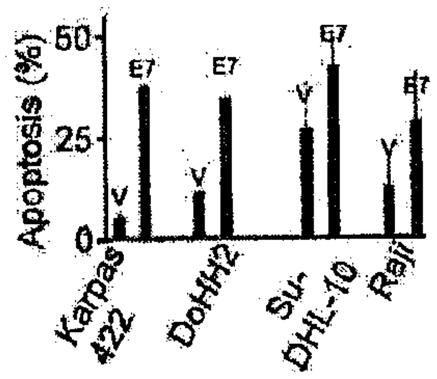
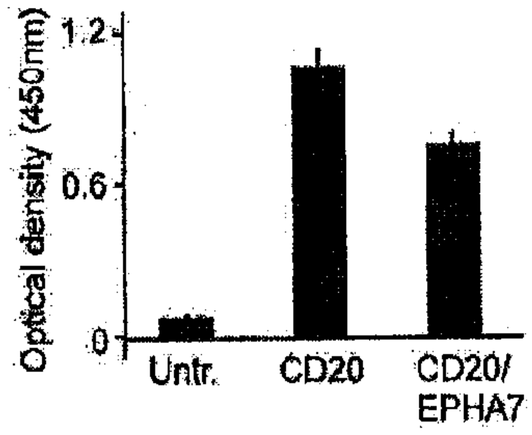
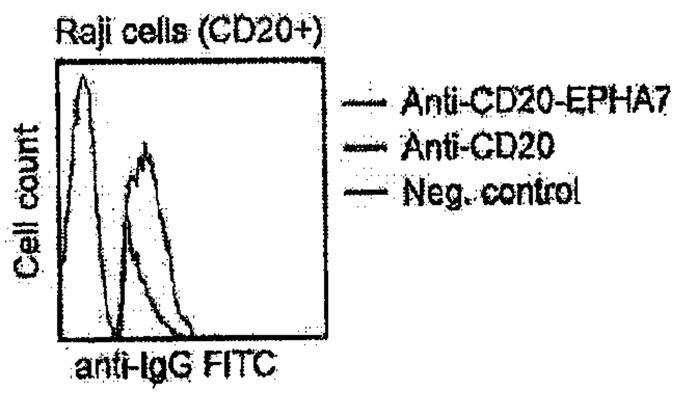

Apoptosis (%)
50
25
0
E7
V
Karpas 422
DoHH2
Su-DHL-10
Raji

Figure 23

a



b



c

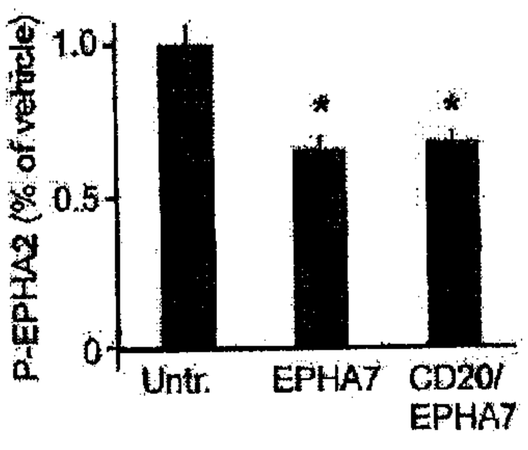
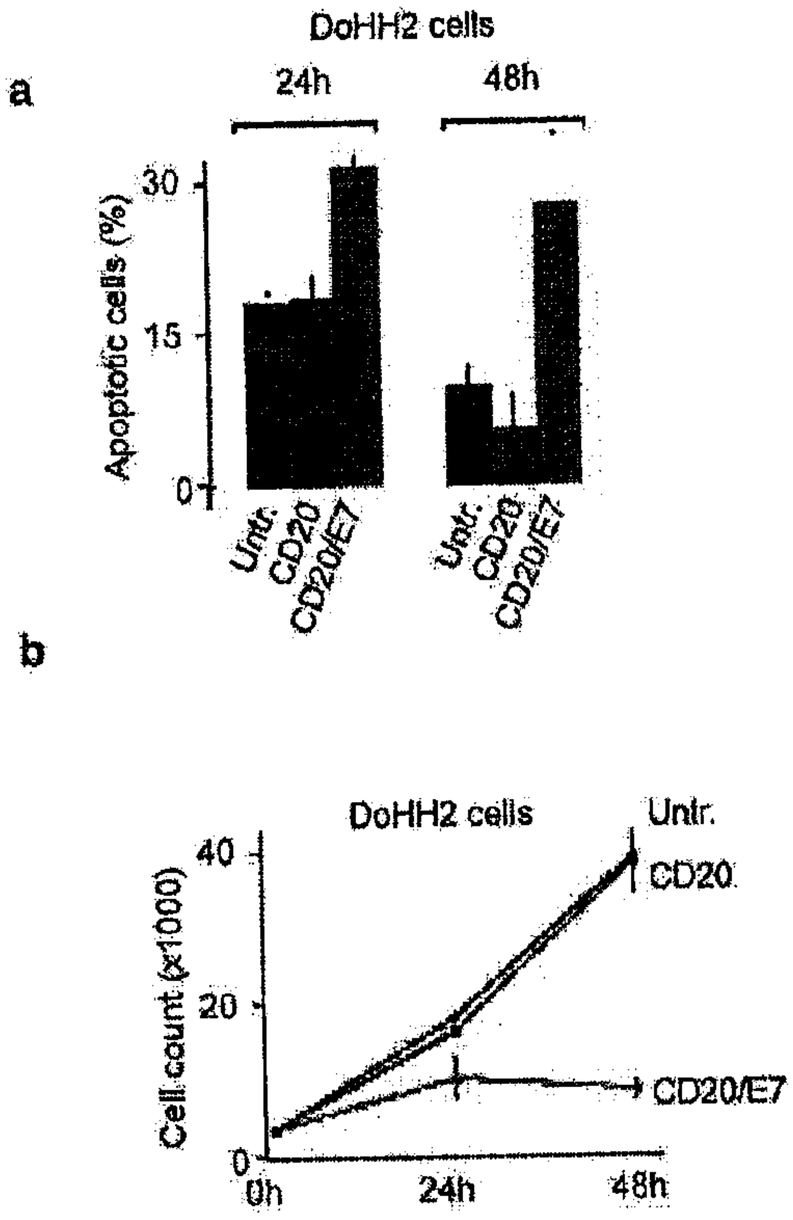


Fig. 24


a
DoHH2 cells
24h
48h
Apoptotic cells (%)
30
15
0
Untr.
CD20
CD20/E7
Untr.
CD20
CD20/E7
b
DoHH2 cells
Untr.
CD20
CD20/E7
Cell count (x1000)
40
20
0
0h
24h
48h